

AD-A043 980

WASHINGTON UNIV SEATTLE DEPT OF MINING METALLURGICAL--ETC F/G 20/5
OPTICAL PROPERTIES OF EUROPIUM-DOPED POTASSIUM CHLORIDE LASER W--ETC(U)
JUL 77 T G STOEBE, J B WOLFENSTINE AF-AFOSR-2977-76

UNCLASSIFIED

AFOSR-TR-77-1003

NL

1 of 1
ADA043980



END
DATE
FILMED
9-77
DDC

12
B-5

AFOSR-TR- 77 - 1003

AD A 043980

Optical Properties of Europium-Doped
Potassium Chloride Laser Window Materials

T. G. Stoebe and J. B. Wolfenstine

Department of Mining, Metallurgical and Ceramic Engineering
University of Washington
Seattle, Washington

Gra AFOSR GRANT 76-2977

Final Report
30 June 1977

Period Covered: 1 January 1976 - 30 June 1977

Prepared for: Electronic and Solid State Sciences Division
Air Force Office of Scientific Research
Washington, D. C. 20332

DDC
RECEIVED
SEP 12 1977
A

Approved for public release;
distribution unlimited.

TO INU.
IDC FILE COPY.

AIR FORCE OFFICE OF SCIENTIFIC RESEARCH (AFSC)
NOTICE OF TRANSMITTAL TO DDC
This technical report has been reviewed and is
approved for public release IAW AFR 190-12 (7b).
Distribution is unlimited.
A. D. BLOSE
Technical Information Officer

19 REPORT DOCUMENTATION PAGE		READ INSTRUCTIONS BEFORE COMPLETING FORM	
1. REPORT NUMBER AFOSR-TR-77-1003	2. GOVT ACCESSION NO.	3. RECIPIENT'S CATALOG NUMBER	
4. TITLE (and Subtitle) Optical Properties of Europium-Doped Potassium Chloride Laser Window Materials.	5. TYPE OF REPORT & PERIOD COVERED Final Report 1 Jan 76 to 30 June 77		
7. AUTHOR(s) T. G. Stoebe and J.B. Wolfenstine	6. PERFORMING ORG. REPORT NUMBER		
9. PERFORMING ORGANIZATION NAME AND ADDRESS Department of Mining, Metallurgical and Ceramic Engineering, FB-10, University of Washington, Seattle WA, 98195	8. CONTRACT OR GRANT NUMBER(s) AFOSR-76-2977		
11. CONTROLLING OFFICE NAME AND ADDRESS Electronic & Solid State Sciences Division (NE) Air Force Office of Scientific Research Washington, D.C. 20332	10. PROGRAM ELEMENT, PROJECT, TASK AREA & WORK UNIT NUMBERS 61102F / 2306/C2		
14. MONITORING AGENCY NAME & ADDRESS (if different from Controlling Office) 25p.	12. REPORT DATE 31 July 1977		
	13. NUMBER OF PAGES 23		
	15. SECURITY CLASS. (of this report) Unclassified		
16. DISTRIBUTION STATEMENT (of this Report) Approved for public release; distribution unlimited.			
17. DISTRIBUTION STATEMENT (of the abstract entered in Block 20, if different from Report) AF-AFOSR-2977-76			
18. SUPPLEMENTARY NOTES			
19. KEY WORDS (Continue on reverse side if necessary and identify by block number) Laser windows Europium Alkali halides Potassium chloride			
20. ABSTRACT (Continue on reverse side if necessary and identify by block number) A study of lattice defect equilibria in the KCl:Eu crystal KC.01ECH97, produced by the Harshaw Chemical Company as part of the AFML laser window development program, has been undertaken using optical absorption, electron spin resonance and ionic conductivity. These techniques reveal that the predominant specie of the Eu ion is Eu⁺⁺, in the form of Eu⁺⁺-vacancy complexes at room temperature. The ultraviolet absorption bands of Eu⁺⁺ that occur at 243 and 330 nm have been used to allow a non-destructive determination of the Eu⁺⁺ content. The room			

409464

13

UNCLAS

Unclassified

SECURITY CLASSIFICATION OF THIS PAGE(When Data Entered)

20.

temperature absorption coefficient of the 243 and 330 nm bands have been calibrated by polarographic and ionic conductivity, such that the relationship between the optical absorption coefficient, α , and Eu^{++} content is given by:

$$\text{Mole \% Eu}^{++} = 4.3 \times 10^{-4} \alpha.$$

alpha

.00043 alpha.

Unclassified

SECURITY CLASSIFICATION OF THIS PAGE(When Data Entered)

TABLE OF CONTENTS

SECTION	PAGE
I. INTRODUCTION	1
II. BACKGROUND	2
III. EXPERIMENTAL	6
IV. RESULTS AND DISCUSSION	8
V. CONCLUSIONS	11
REFERENCES	12

ADDITIONAL	
NTIS	Write Sample <input checked="" type="checkbox"/>
DDC	Full Content <input type="checkbox"/>
UNANNOUNCED	<input type="checkbox"/>
JUSTIFICATION	
BY	
DISTRIBUTION AVAILABILITY CODES	
Dist.	AVAIL. and/or SPECIAL
<i>A</i>	

LIST OF ILLUSTRATIONS

FIGURE		PAGE
1	Optical absorption spectrum of KCl:Eu^{++} at room temperature. Spectrum H is from the heel section and spectrum C is from the cone section of sample KC.01ECH97.	14
2	Concentration vs. crystal location determined using absorption and polarographic results, from ref. 10. Schematic sections at heel and cone show sample locations and grain boundaries(see also Fig. 3).	15
3	Sectioning plan for Harshaw-grown ingot KC.01ECH97. See Figure 2 for specific sample locations in cone and heel sections.	16
4	Ionic Conductivity plots of pure KCl and KCl:Eu crystals from the heel and cone sections of Harshaw-grown ingot KC.01ECH97. Sample numbers from Fig. 2.	17
5	Absorption coefficient of the 243 nm band versus Eu^{++} concentration, as determined by ionic conductivity. The slope, determined by least squares curve fitting, is 0.234; the slope inverse gives proportionality constant in eq. [5].	18
6	Same as Fig. 1 with addition of points \bullet , which represent Eu^{++} concentration determined by ionic conductivity (Fig. 5) compared to polarographic Eu-ion content.	19
7	Esr spectrum for KCl:Eu powder at room temperature.	20

SECTION I

INTRODUCTION

Recent advances in infrared laser technology have demanded the development of a suitable window material for the high powered CO₂ gas laser system. The window materials under consideration are primarily alkali halides, with the most promising of these being NaCl, KBr, NaBr and KCl(1). These alkali halides are preferred in that they have very low optical absorption coefficients over a wide portion of the infrared spectrum. However they do have the drawback that in their single crystal state they are quite weak. Therefore in order to use these alkali halides for window materials it is important to increase their strength without decreasing their transparency. Some of the strengthening methods being investigated are recrystallization, alloying and radiation hardening (1). In KCl, one of the main strengthening methods used involves alloying it with europium (Eu).

In order for the europium-doped KCl (KCl:Eu) material to be used in a laser window system, either in single crystalline polycrystalline form, it is important to characterize its lattice defect state and to relate the lattice defect structure to the optical properties of the material. This characterization should include the determination of the Eu impurity distribution throughout the crystal, the nature of the charge and state of the Eu impurity content. These crystal characterization goals are the basis of this present work in KCl:Eu single crystals.

SECTION II

BACKGROUND

Various studies in KCl:Eu have indicated the presence of Eu^+ , Eu^{++} , and Eu^{+3} ions in this material. The predominant ion present at room temperature appears to be Eu^{++} present in the form of Eu^{++} -vacancy dipoles (2-5).

The Eu^{++} ion has two characteristic ultraviolet absorption bands that are due to electronic transitions from the $4f^7$ ground state to the e_g and t_{2g} components of the $4f^6 5d^1$ configuration, with the former being at higher energy (6). These bands occur at 243 nm and at 330 nm. A typical room temperature absorption spectrum of the KCl:Eu⁺⁺ is shown in Fig. 1, where the more intense curve (H) is from the heel section and the lower curve (C) is from the cone section Harshaw KCl:Eu crystal KC.01ECH97. The 3300 Å band consists of a staircase structure that can be partially resolved at room temperature; at low temperatures it is composed of peaks at 3290, 3430 and 3640 Å (7). The 2400 Å band can only be resolved at low temperatures; at 77°K it consists of five individual peaks at 2340, 2400, 2440, 2510 and 2580 Å (7). All of the samples from our KCl:Eu crystal showed the blue luminescent color characteristic of Eu^{++} (6).

The absorption spectrum of trivalent Eu ions has been observed only in europium salts (8) and in $\text{LaCl}_3:\text{Eu}^{+++}$ (9). The principal absorption lines that are of interest are at 5790, 5260, 4650 and 3960 Å. Of these, the absorption at 4650 Å has been reported as being about twice as intense as the others, while the presence of the absorption of 5790 Å seems questionable. Stoebe and Spry (10) made attempts to observe the Eu^{+++} absorption bands 5790, 5260, 4650 and 3960 Å in as-received KCl:Eu crystals by annealing the crystals at 650°C for 4 hours and then rapidly cooling them to room temperature (cooling accomplished in about 30 sec.). Honeywell Corporation

development work (1) had indicated that KCl:Eu becomes brittle after annealing at 650°C in air; Honeywell speculated that this was caused by the oxidation of Eu^{++} to Eu^{+++} . However, no Eu^{+3} absorption bands were observed by Stoebe and Spry (10) and any change in the Eu^{++} content (243 nm peak) was small and virtually undetectable. These observations suggest that the concentration of Eu^{+++} as compared to the total Eu concentration is negligible.

The optical absorption bands of the Eu^{++} (243 nm and 330 nm), if calibrated, can allow for a non-destructive determination of the Eu^{++} content. Stoebe and Spry (10) calibrated the peak absorption coefficient of the 243 nm band against the Eu concentration as determined by the Honeywell polarographic analysis (11). The 243 nm band was chosen rather than the 330 nm band, since from Fig. 1, the 243 nm band has less structure at room temperature. A linear relationship was obtained as follows:

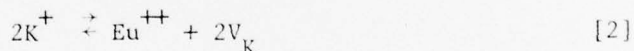
$$\text{mole \% Eu} = 4.2 \times 10^{-4} \alpha \quad [1]$$

where α is the peak absorption coefficient of the 243 nm band in cm^{-1} at room temperature. The relative comparison of optical absorption results and polarographic analysis using eq[1] is shown in Fig. 2 (10).

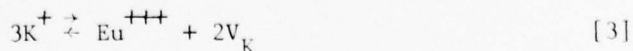
Using peak absorption coefficients and polarographic data, Stoebe and Spry (10) were able to determine the Eu impurity distribution in the edge, heel and cone regions of the KCl:Eu crystal KC.01ECH97. They found that the Eu^{++} content through the crystal generally followed the expected variations for an impurity with a distribution coefficient of less than one, except for the rise in concentration near the surface. The initial Eu content in the melt was 100 mole ppm; this decreased to indicated concentrations in the crystal on the order of 30 mole ppm near the cone and 60 mole ppm near the heel, as shown in Fig. 2. The relative intensities of the absorptions in Fig. 1 also indicate the variation of Eu^{++} content from heel (H) to cone (C).

Ionic conductivity is another technique that may be used to investigate lattice defect configurations and divalent (or trivalent) ion concentrations. Ionic conductivity data can thus provide another calibration check on the Eu^{++} content.

A simple theory of ionic conductivity, which is adequate for most of our work, has been well summarized by Lidiard (12) and Suptitz and Tetlow (13). The main point is that the variation of the concentration of free cation vacancies as a function of temperature for doped crystals enables the calculation of the impurity content. Of the three possible species of the Eu-ion present in KCl:Eu , only the Eu^{++} and the Eu^{+++} can be detected by ionic conductivity, since only these two ion valences increase the concentration of free cation vacancies. If Eu^+ is introduced into the KCl lattice to replace K^+ , no extra cation vacancy is needed to maintain charge neutrality and hence Eu^+ cannot be detected by ionic conductivity. However, if Eu^{++} is introduced into the KCl lattice to replace K^+ an extra cation vacancy is also created to maintain charge neutrality, according to the charge balance equation,



where V_K indicates a cation vacancy. This extra cation vacancy can contribute to ionic conductivity and allows detection of Eu^{++} ions. If Eu^{+3} is introduced into the KCl to replace K^+ , 2 extra cation vacancies are also created to maintain charge neutrality, according to the charge balance equation,



Hence these extra cation vacancies can also contribute to ionic conductivity and allow detection of the Eu^{+++} ion.

Ionic conductivity is usually plotted as $\ln \sigma T$ ($\text{ohm}^{-1} \text{cm}^{-1} \text{K}$) versus $1/T$ (K^{-1}). For our purpose, only regions I and II of the conductivity plot

need be considered. In region I the concentration of cation vacancies is governed only by the thermal statistics of the lattice and is independent of the impurity doping level. The slope of the $\ln \sigma T$ vs. $1/T$ plot in region I is $(H_s/2 + H_m)$, where H_s is the Schottky energy of formation, and H_m is the energy of motion of the cation vacancy. Region II is known as the extrinsic region and is where the concentration of cation vacancies is equal to the concentration of divalent impurities; the slope in this region is H_m . The temperature at which regions I and II intersect is known as the knee temperature and at this point the concentration of intrinsic cation vacancies equals the concentration of extrinsic vacancies (concentration of divalent impurities). Thus the determination of the knee temperature and the slopes of regions I and II allows the calculation of the concentration of divalent impurities present.

Electron spin resonance (esr) in Eu is due to inner shell (4f) electrons and should not be influenced by valence changes which involve outer shell (5d, 6s) electrons. Esr can be used to determine Eu-ion environments, however, especially as related to the presence of Eu-vacancy pairs (2,3). Hence, esr is one of the principal methods used to demonstrate that Eu^{++} paired with one vacancy is the predominant defect present at room temperature in KCl:Eu .

SECTION III

EXPERIMENTAL

The KCl:Eu crystals used in this study were from KCl:Eu ingot KC.01ECH97 (10), a 17-inch diameter by 7-inch high single crystal grown by the Harshaw Chemical Company for the AFML-monitored laser window development program. The sectioning plan for this ingot is shown in Fig. 3. The KCl:Eu samples were taken from locations shown in more detail in Fig. 2; samples from the heel (last part to solidify) are shown in Fig. 2 (10), as H2 and H4, while samples from the cone section (first part to solidify) are shown in Fig. 2 as C2 and C4. Also available were several Harshaw-grown undoped KCl single crystals.

The techniques used to investigate the crystals consisted of optical absorption, electron paramagnetic resonance and ionic conductivity. Polarographic analysis of the Eu-ion content was obtained by Honeywell, Inc. (11) on samples immediately adjacent to those used for the current work. The polarographic analysis results for heel and cone scans along with the earlier optical absorption determinations of Eu-ion content have been shown in Fig. 2.

The samples used for optical absorption measurements were cleaved to thicknesses 5 mm and 1 mm. Samples were used in the unpolished condition; however, care was taken so that the part of the crystal in the beam contained no cleavage steps. Some of the crystals that were used in the unpolished condition were also mechanically polished to an optical finish using 0.6 μm alumina polishing powder and compared to measurements made in the unpolished condition; no differences were observed. All optical absorption measurements were made on a Cary-14 spectrophotometer at room temperature and the optical absorption coefficient was calculated from

the optical density and the thickness of the crystal. The effect of reflectance in KCl is approximately 3.5% and therefore can be neglected; thus, α can be calculated from the peak absorption coefficient (14) using the relation:

$$\alpha = \frac{2.303(O.D.)}{t} \quad [4]$$

Here t is the sample thickness and O.D. represents the optical density of the sample. Optical absorption measurements were also made on a few of the Harshaw-grown undoped KCl single crystals for comparative purposes.

Ionic conductivity measurements were made using an A.C. method at 1592 Hz using a Wayne-Kerr Universal Bridge which measured both conductance and capacitance of the sample. Conductivity values were determined by multiplying the measured conductance by L/A , where L is the length of the sample and A is the cross sectional area of the sample. The crystal was coated with a colloidal graphite and then mounted between two nickel electrodes in the conductivity jig.(15). The conductivity jig was placed inside a horizontal Vycor tube which was heated by a Marshall furnace. The furnace temperature of the crystal was measured by means of a chromel-alumel thermocouple placed next to the crystal and connected to a digital volt meter. Before making the conductivity measurements, the crystals were annealed for 1 hr. at 420°C to allow for sample equilibrium. During the annealing treatment and the conductivity measurements the furnace was continually flushed with dry helium gas. The conductivity measurements were made in equilibrium on heating from 420°C to 750°C at 25°C intervals.

The electron spin resonance (esr) work done was qualitative in nature. The esr measurements were made at room temperature at X-band using a Varian V-4502-EPR spectrometer with 100 KC field modulation. For the single crystals the spectra were recorded with the applied magnetic field along the $\langle 110 \rangle$ directions. Spectra from a KCl:Eu crystal that had been crushed and ground to a fine powder ($<100\mu\text{m}$) were also recorded at room temperature.

SECTION IV

RESULTS AND DISCUSSION

Ionic conductivity plots of the KCl:Eu crystals from samples H2, H4, C2 and C4 are shown in Fig. 4 where the intrinsic slope is determined from that of the Harshaw crystals. The slope in region II, H_m , is 0.81 eV from crystal C2 (16). This value seems high compared to some recent work (17-19) but agrees fairly well with earlier studies (20-22). From the slope of region I and this value of H_m , H_s was determined as 2.56 eV. This agrees well with recent work. Using this value and the knee temperatures, the Eu^{++} content of these KCl:Eu crystals was then determined.

Assignment of a Eu^{++} content from the above is valid only if no Eu^{+3} contributes to the ionic conductivity data. Again the optical absorption bands at 5790, 5260, 4650 and 5960 Å were checked for Eu^{+3} absorptions. As with the work of Stoebe and Spry (10), none were observed.

The optical absorption coefficients at room temperature of both the 243 and 330 nm band were calculated for the KCl:Eu crystals H2, H4, C2 and C4. The optical absorption coefficient of the 243 nm band is calibrated against the Eu^{++} content determined by ionic conductivity using a least squares analysis, as shown in Fig. 5. The result indicates a linear relationship between these two measurements such that:

$$\text{mole \% Eu}^{++} = 4.3 \times 10^{-4} \alpha \quad [5]$$

This result agrees well with the work of Stoebe and Spry (10) and is probably more accurate than their value. This result may also be compared to the polarographic analysis of the adjacent samples as in Fig. 6. The comparison agrees to within 10% in three of the locations but varies 25% at the fourth (Sample H4). The reasons for this discrepancy are not clear.

When the optical absorption coefficient of the 330 nm band is

calibrated against Eu^{++} content determined by ionic conductivity, a linear relationship exists as follows:

$$\text{mole \% Eu}^{++} = 4.5 \times 10^{-4} \alpha \quad [6]$$

This compares well with the calibration of the 243 nm band given in eq. [5].

The result in eq.[5] may also compare to the results of Sill et al.(23), who used atomic absorption spectroscopy to measure the Eu^{++} impurity content. Compared to the optical absorption coefficient of the 243 nm band, Sill et al. obtained a proportionality factor that was 8 higher than that in eq. [5]. This may indicate the presence of additional Eu in their crystals, present either as Eu^+ or in a state of agglomeration, neither of which would be measured using ionic conductivity. However, this discrepancy is not seen in the polarographic analysis of our samples, noted above. Causes for this discrepancy are being investigated further using the other lattice defect investigative techniques.

The esr spectrum when the magnetic field is along $\langle 100 \rangle$ is quite complex and at room temperature consisted of 168 lines. Comparing the room temperature spectra to those in the literature (2,3,34), where similar spectra were studied in terms of a cation vacancy at a nearest neighbor site next to the Eu^{++} ion, suggests that at room temperature the Eu^{++} ion is indeed in the form of Eu^{++} -vacancy dipoles.

The esr spectra of the KCl:Eu powder at room temperature is shown in Fig. 7. The powder spectra shows a much reduced number of lines as compared to the single crystal spectra; this is expected because in the powder the spectra is a superposition of a large number of spectra resulting from all possible orientations of the applied magnetic field with axis of the crystal. Since the powder is composed of many randomly oriented crystals, the total spectrum is independent of the direction of the external field. Thus the angular terms drops out in the powder sample.

The observed powder spectrum contains 12 lines. These lines are probably due to the hyperfine splitting of Eu ion isotopes Eu^{151} and Eu^{153} each with spin (I) equal to 5/2. Further work is needed to determine the potential use of powder esr spectra in defect studies in KCl:Eu .

SECTION V
CONCLUSIONS

The 243 and 330 nm absorption bands in KCl:Eu, when calibrated by polarographic analysis and ionic conductivity data, can yield a non-destructive determination of Eu^{++} content in KCl:Eu laser window materials. The concentration of Eu^{+3} is negligible when compared to the total Eu concentration in the KCl:Eu samples studied. The results also indicate that at room temperature the Eu^{++} is in the form of Eu^{++} -vacancy dipoles.

The discrepancy between the Eu content determined by polarographic analysis, by atomic absorption and by ionic conductivity may be due to cation vacancies that are trapped by some type of complex that would not allow detection by ionic conductivity, or by the presence of some of the Eu in the form of Eu^{+} ions. These possibilities are being investigated further.

REFERENCES

1. W. B. Harrison, Halide Material Processing for High Power Infrared Laser Windows, Final Technical Report AFML-TR-75-104, Honeywell, Inc., July 1975.
2. R. Rohrig, Phys. Lett. 16, 20 (1965)
3. P.G. Nair, K. V. Lingam and R. Venkataraman, J. Phys. Chem. Solids 29, 2183(1968)
4. G. Aguliar, E. Munoz, H. Murrieta, L.A. Boatner, and R.W. Reynolds J. Chem. Phys. 60, 4665 (1975)
5. V.M. Maevskii, E.N. Kalabokhova, A.N. Zhukov and B.N. Krulilovskii, Sov. Phys.-Solid State 17, 150 (1975)
6. R. Reisfield and A. Glasner, J. Opt. Soc. Amer. 54, 331 (1964)
7. B.V.R. Chowdrai and N. Itoh, Phys. Stat. Sol. (b) 46, 549 (1971)
8. B.F. Kim and H.W. Moos, Phys. Rev. 161, 869 (1967)
9. L.G. DeShazer and G. H. Dieke, J. Chem. Phys. 38, 2190 (1963)
10. T.G. Stoebe, R.J. Spry and J.F. Lewis, Optical Properties of Europium-doped Potassium Chloride Laser Window Materials, Technical Report AFML-TR-76-20, April 1976
11. W.B. Harrison, Alkali Halide Materials for High Power Infrared Laser Windows, Final Technical Report AFML-TR-76-106, Honeywell Inc., June 1976
12. A. B. Lidiard, Handbuch der Physik, edited by S. Flosse (Springer-Verlag, Berlin 1957) Vol. 20, p. 246
13. P. Süptitz and S. Tetlow, Phys, Stat. Sol., 23, 9 (1967)
14. P.D. Townsend and J.C. Kelly, Colour Centers and Imperfections in Insulators and Semiconductors, Sussex University Press, London (1973)
15. H. Vora, Ph. D. Thesis, University of Washington (1974)
16. T. G. Stoebe and P. L. Pratt, Proc. British Ceramic Soc. 9, 181 (1967)
17. J. Beaumont and P. Jacobs, J. Chem. Phys. 45, 149 (1966)
18. S. Chandra and J. Rolfe, Can. J. Phys. 48, 412 (1970)
19. R. Fuller and C. Marquardt, Phys. Rev. 176, 1036 (1968)

20. M. Beniere, F. Beniere and M. Chemla, J. Chem. Phys. 67, 1312 (1970)
21. R. Dreyfus and A. Nowick, J. Appl. Phys. 33, 473 (1962)
22. A. Allnatt and P. Jacobs, Trans Faraday Soc. 58, 116 (1962)
23. E. L. Sill, J.J. Martin and Z. Al. Shaieb, Phys. Stat. Sol. (A) 39, K131 (1977)
24. S. D. Pawdey, J. Chem. Phys. 47, 3094 (1967)

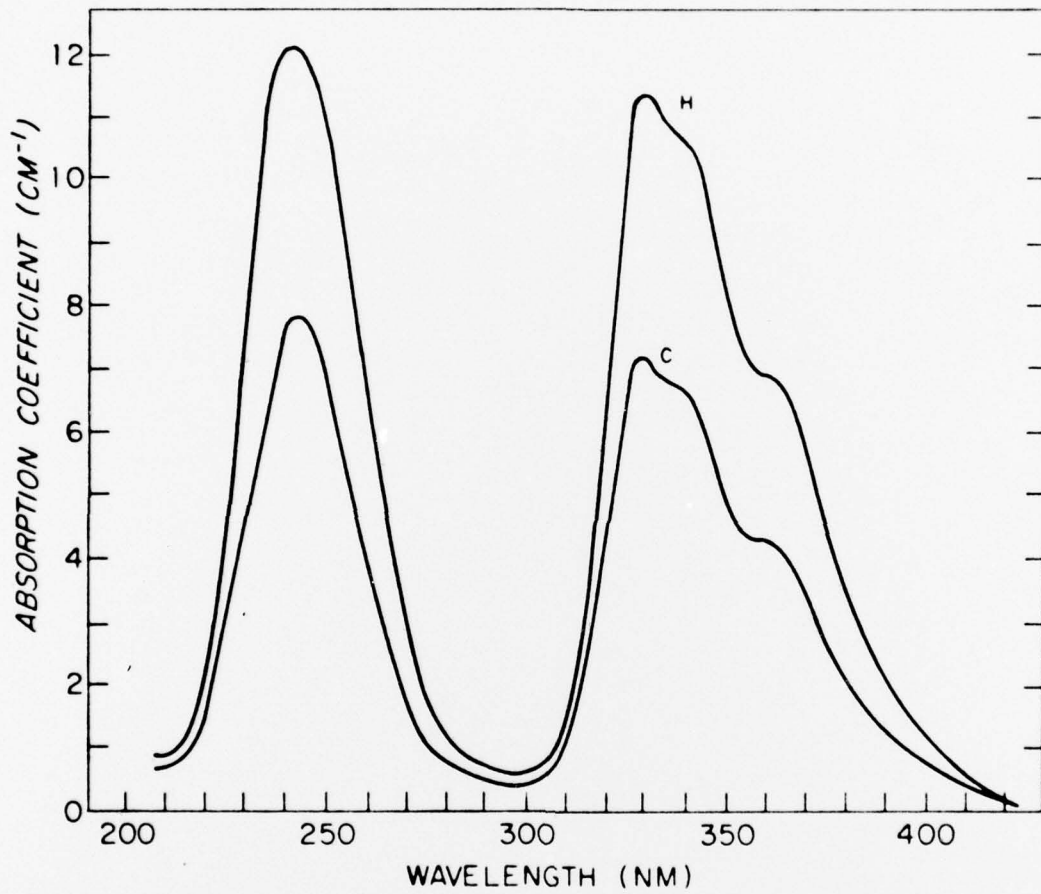


Figure 1. Optical absorption spectrum of KCl:Eu^{++} at room temperature. Spectrum H is from the heel section and spectrum C is from the cone section of sample KC.01ECH97.

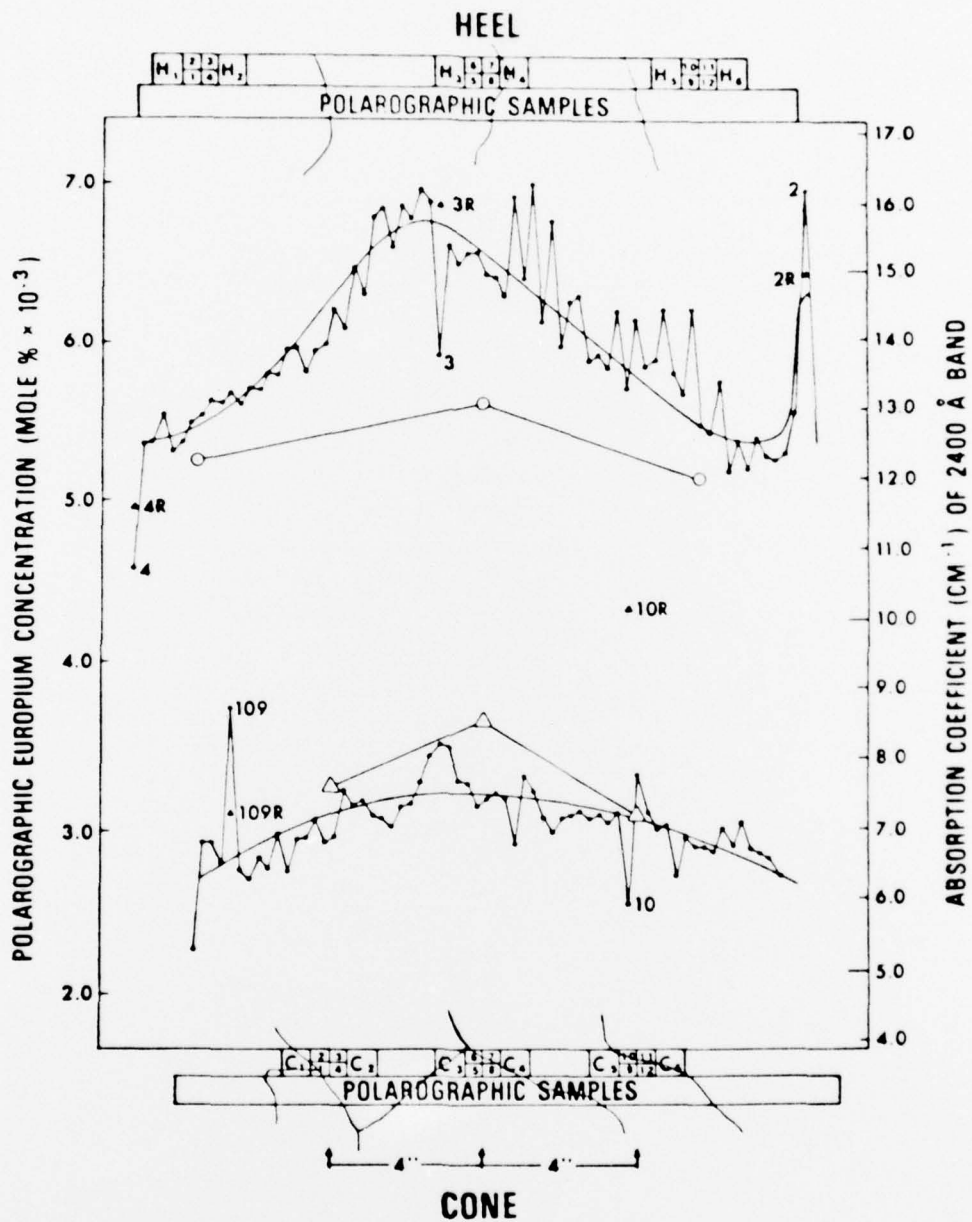


Figure 2. Concentration vs. crystal location determined using absorption and polarographic results, from ref. 10. Schematic sections at heel and cone show sample locations and grain boundaries. (See also Fig. 3).

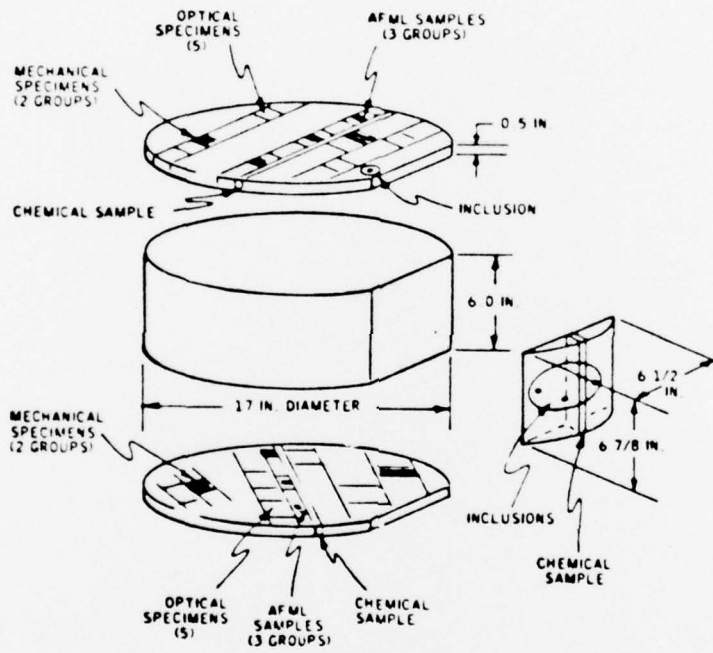


Figure 3. Sectioning plan for Harshaw-grown ingot KC.01ECH97. See Figure 2 for specific sample locations in cone and heel sections.

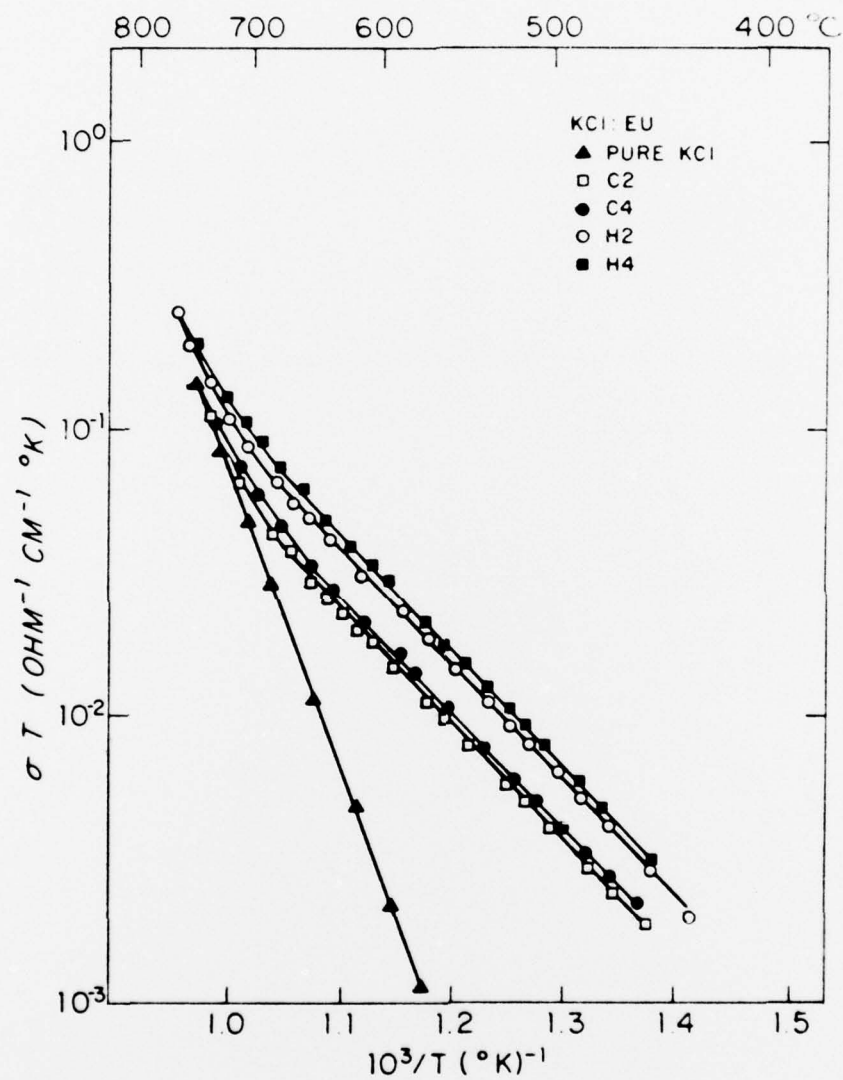


Figure 4. Ionic Conductivity plots of pure KCl and KCl:Eu crystals from the heel and cone sections of Harshaw-grown ingot KC.01ECH97. Sample numbers from Fig. 2.

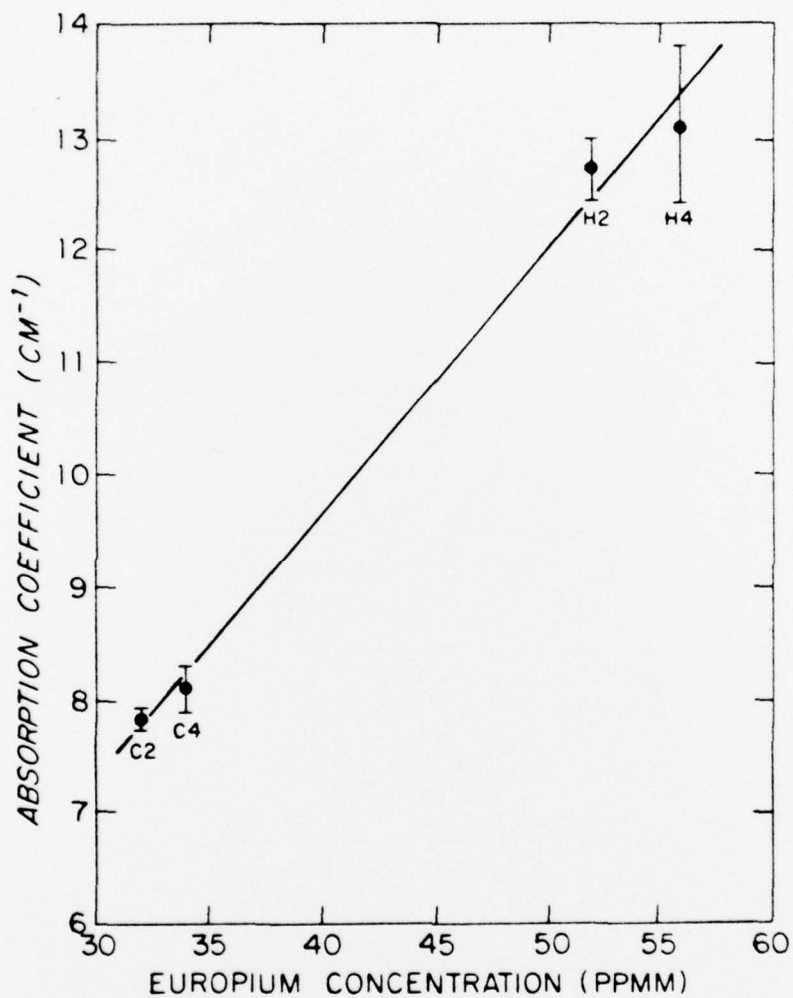


Figure 5. Absorption coefficient of the 243 nm band versus Eu^{++} concentration, as determined by ionic conductivity. The slope, determined by least squares curve fitting, is 0.234; the slope inverse gives proportionality constant in eq. [5].

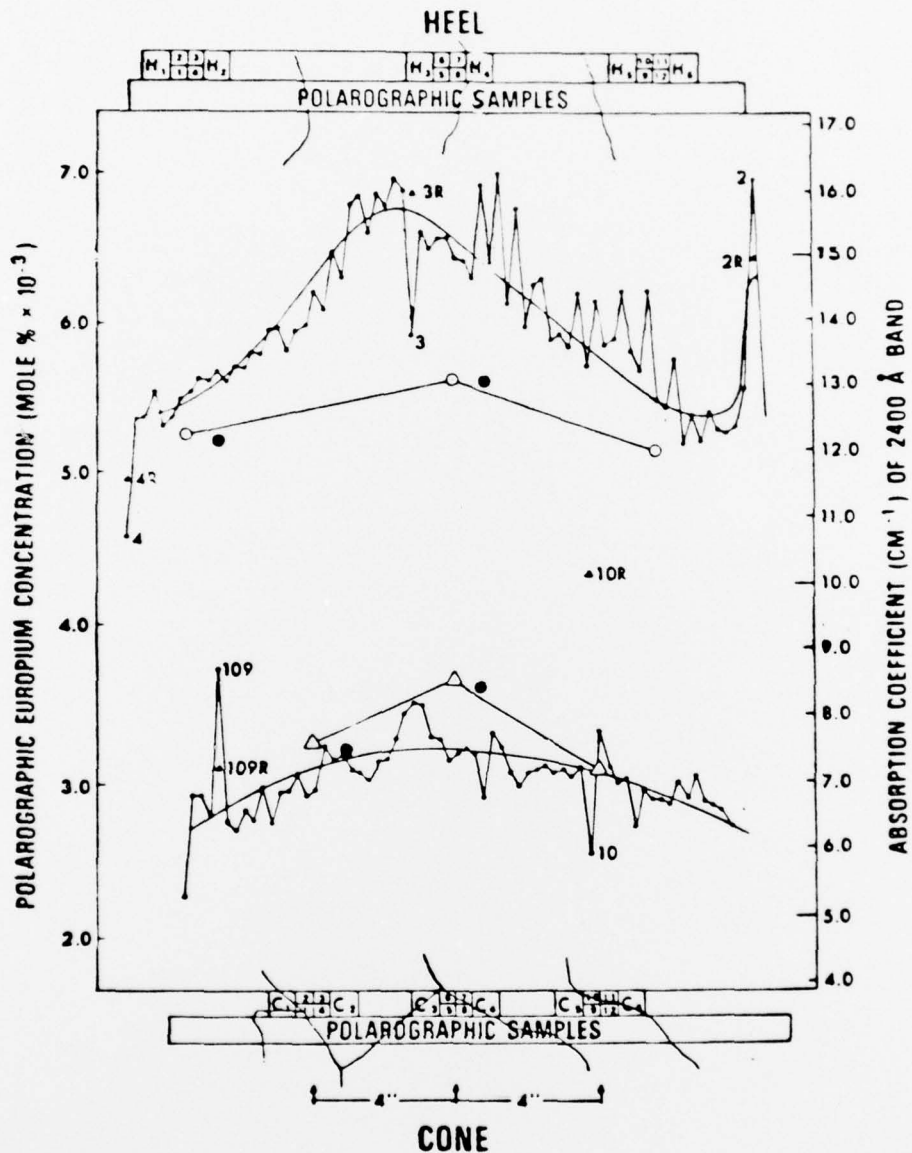


Figure 6. Same as Fig. 1 with addition of points •, which represent Eu^{++} concentration determined by ionic conductivity (Fig. 5) compared to polarographic Eu -ion content.

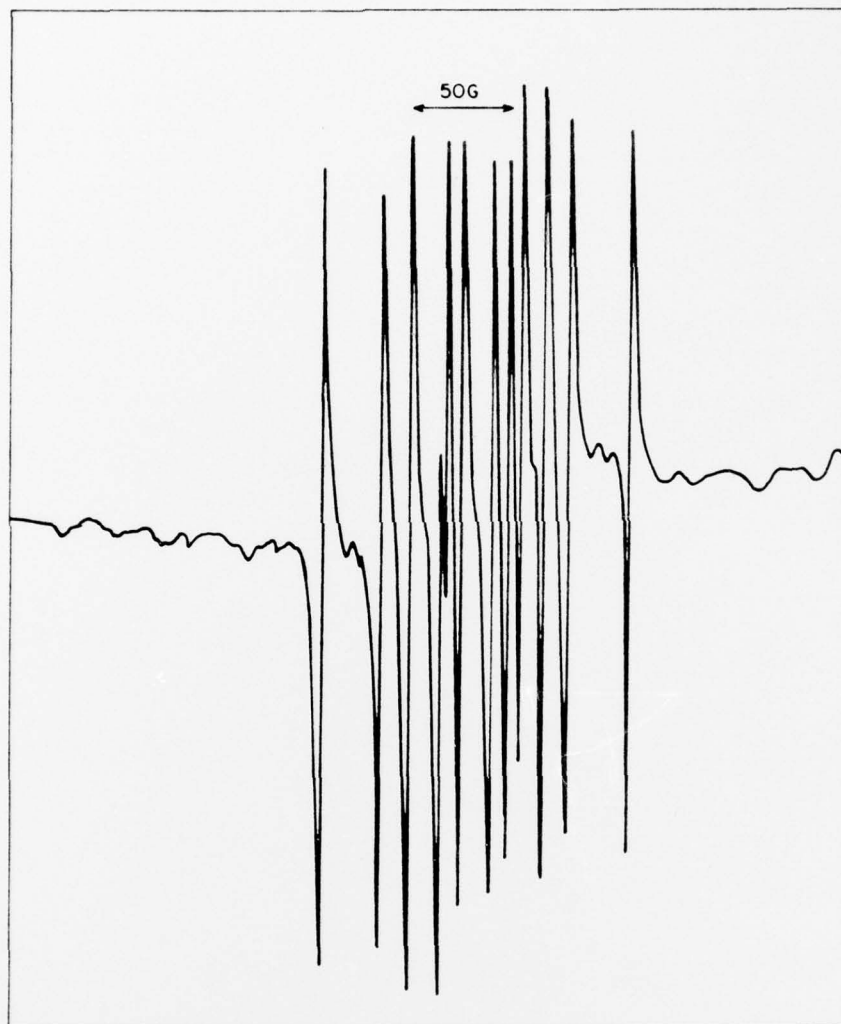


Figure 7. ESR spectrum for KCl:Eu powder at room temperature.